

Exciton-polaritons in a 2D hybrid organic-inorganic perovskite microcavity with the presence of optical Stark effect

Kenneth Coker, Chuyuan Zheng(郑楚媛), Joseph Roger Arhin, Kwame Opuni-Boachie Obour Agyekum, and Weili Zhang(张伟利)

Citation: Chin. Phys. B, 2024, 33 (**3**): 037102. DOI: 10.1088/1674-1056/ad1484
Journal homepage: http://cpb.iphy.ac.cn; http://iopscience.iop.org/cpb

What follows is a list of articles you may be interested in

Structural, electronic and magnetic properties of Fe-doped strontium ruthenates

Nan Liu(刘楠), Xiao-Chao Wang(王晓超), and Liang Si(司良)
Chin. Phys. B, 2023, 32 (**11**): 117101. DOI: 10.1088/1674-1056/ad0112

Infrared optical absorption of Fröhlich polarons in metal halide perovskites

Yu Cui(崔钰), Xiao-Yi Liu(刘晓逸), Xu-Fei Ma(马旭菲), Jia-Pei Deng(邓加培), Yi-Yan Liu(刘怡言), and Zi-Wu Wang(王子武)
Chin. Phys. B, 2023, 32 (**9**): 097102. DOI: 10.1088/1674-1056/aca7f0

Electronic structure of cuprate-nickelate infinite-layer heterostructure

Dachuan Chen(陈大川), Paul Worm, Liang Si(司良), Chunxiao Zhang(张春小), Fenglin Deng(邓凤麟), Peiheng Jiang(蒋沛恒), and Zhicheng Zhong(钟志诚)
Chin. Phys. B, 2023, 32 (**8**): 087105. DOI: 10.1088/1674-1056/acd368

Doublet luminescence due to coexistence of excitons and electron-hole plasmas in optically excited $CH_3NH_3PbBr_3$ single crystal

Jie Wang(王杰), Guang-Zhe Ma(马广哲), Lu Cao(曹露), Min Gao(高敏), and Dong Shi(石东)
Chin. Phys. B, 2022, 31 (**4**): 047104. DOI: 10.1088/1674-1056/ac29b5

High-throughput computational material screening of the cycloalkane-based two-dimensional Dion—Jacobson halide perovskites for optoelectronics

Guoqi Zhao(赵国琪), Jiahao Xie(颉家豪), Kun Zhou(周琨), Bangyu Xing(邢邦昱), Xinjiang Wang(王新江), Fuyu Tian(田伏钰), Xin He(贺欣), and Lijun Zhang(张立军)
Chin. Phys. B, 2022, 31 (**3**): 037104. DOI: 10.1088/1674-1056/ac4036

Exciton–polaritons in a 2D hybrid organic–inorganic perovskite microcavity with the presence of optical Stark effect

Kenneth Coker[1,2], Chuyuan Zheng(郑楚媛)[1,†], Joseph Roger Arhin[1], Kwame Opuni-Boachie Obour Agyekum[3], and Weili Zhang(张伟利)[1]

[1] *School of Information and Communication Engineering, University of Electronic Science and Technology of China, Chengdu* 611731, *China*
[2] *Department of Electrical and Electronic Engineering, Ho Technical University, Ho* 00233, *Ghana*
[3] *Telecommunication Engineering Department, Kwame Nkrumah University of Science and Technology, Kumasi* 00233, *Ghana*

(Received 22 October 2023; revised manuscript received 6 December 2023; accepted manuscript online 12 December 2023)

This study investigates the properties of exciton–polaritons in a two-dimensional (2D) hybrid organic–inorganic perovskite microcavity in the presence of optical Stark effect. Through both steady and dynamic state analyses, strong coupling between excitons of perovskite and cavity photons is revealed, indicating the formation of polaritons in the perovskite microcavity. Besides, it is found that an external optical Stark pulse can induce energy shifts of excitons proportional to the pulse intensity, which modifies the dispersion characteristics of the polaritons.

Keywords: exciton–polaritons, perovskite, microcavity, optical Stark effect

PACS: 71.36.+c, 71.20.Nr, 42.70.Qs, 78.20.Bh **DOI:** 10.1088/1674-1056/ad1484

1. Introduction

The layered material class known as two-dimensional (2D) hybrid organic–inorganic perovskites (2D HOIPs) is quickly gaining popularity as a promising semiconductor for optoelectronic and energy-harvesting applications.[1–5] There are several causes for this rise in interest. One of them is the fact that the structure and composition of organic and inorganic components can be changed to alter the physical properties of 2D HOIPs.[6] Furthermore, at ambient temperature, the 2D HOIPs exhibit a high quantum confinement charge that has significant excitonic effects.[7,8]

Whenever an extrinsic trigger, like excitons, collides with light intensively, hybrid particles called polaritons are formed.[9,10] These polaritons have also played a vital role in the development of optoelectronic devices over the last few years.[11,12] Moreover, the behavior of polaritons in 2D HOIPs exhibits remarkable characteristics when confined within a highly reflective structure, such as a distributed Bragg reflector (DBR) mirror.[13] In comparison to more compact designs, the DBR mirror effectively confines light with minimal loss, rendering it highly advantageous for the advancement of polaritonic devices.[14] Leveraging the impact of the optical Stark effect (OSE) on these exciton–polaritons confined between two DBR mirrors becomes particularly promising, given the successful control of polaritons.[15–17] In recent times, researchers have explored the influence of the OSE in 2D WS2[18] monolayers at room temperature and developed an all-optical method to realize topological insulators using OSE within exciton–polariton systems.[19] These studies provide ways to manipulate polaritons through OSE with a large degree of control freedom.

Alternatively, this study introduces 2D HOIP into a microcavity to form exciton–polaritons and focuses on the influence of OSE on the exciton–polaritons. Using both steady and dynamic state analyses, strong coupling between excitons and polaritons is revealed through the observation of Rabi splitting, and the evaluation of polariton branches in the momentum space is analyzed at different strengths of OSE.

2. Methodology

This study presents a setup aimed at analyzing the influence of the OSE on exciton–polaritons within a 2D HOIP active layer. The schematic structure of the setup is illustrated in Fig. 1, featuring exciton–polaritons confined within two highly reflective DBR mirrors. These DBR mirrors are made up of numerous, alternate layers of materials with low and high refractive indices that have been precisely structured to provide high reflectivity at a wavelength band that can confine photons with the same energy to the excitons of the embodied 2D HOIP. The 2D HOIP with a thickness of 0.8 nm, serves as the active material, with the organic layer sandwiched between two inorganic layers, forming the hybrid perovskite.[20] The incorporation of the OSE is applied by illuminating an optical pulse with lower photonic energy to the excitons.

A complex number $m+i\times n$ is used to characterize the refractive index of 2D HOIP.[21] The real part m of the complex number describes how much light is slowed down as it passes through the material. The imaginary component n represents the extinction coefficient, which quantifies the amount of light absorbed by the 2D HOIP. The complex refractive index of

†Corresponding author. E-mail: zcyinuestc@163.com

© 2024 Chinese Physical Society and IOP Publishing Ltd

2D HOIPs is dependent on various factors such as the chemical composition, crystal structure, temperature, and the wavelength of light that passes through it. The complex refractive index can also be influenced by the presence of defects and impurities in the material, which can result in significant changes in the optical properties. The refractive index can be calculated through the complex permittivity, ε_r.[22] As illustrated in Fig. 2, the ability of the 2D HOIP to store electric charges is characterized by its real component ε_m, which represents the permittivity. On the other hand, the energy dissipated due to the absorption of electromagnetic waves is denoted by the imaginary component ε_n, signifying the dielectric loss. The relatively higher permittivity observed in Fig. 2 imparts the 2D HOIP with a distinctive advantage in efficient electric charge storage, making it highly suitable for photovoltaic applications to store electric charges generated from absorbed light.

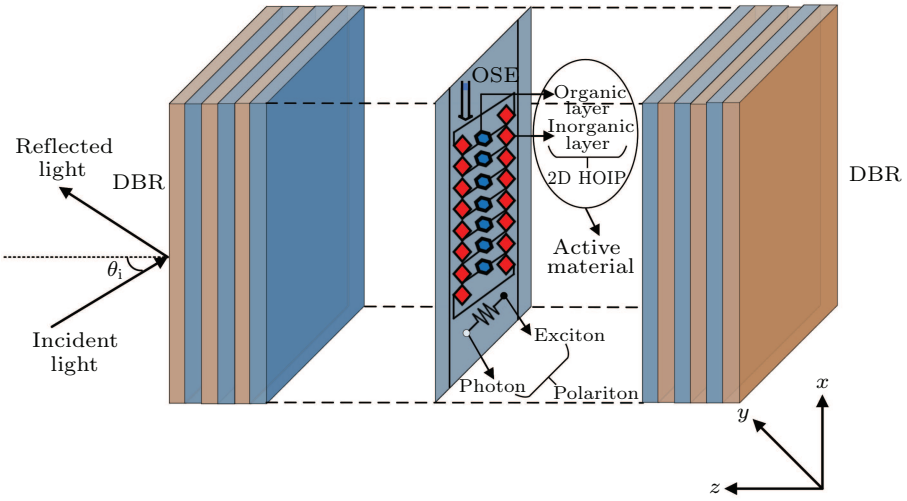


Fig. 1. Structure of the proposed setup. The DBR mirrors serve as the reflective surface, trapping the exciton–polaritons in the microcavity. The 2D HOIP serves as the active material under the influence of OSE.

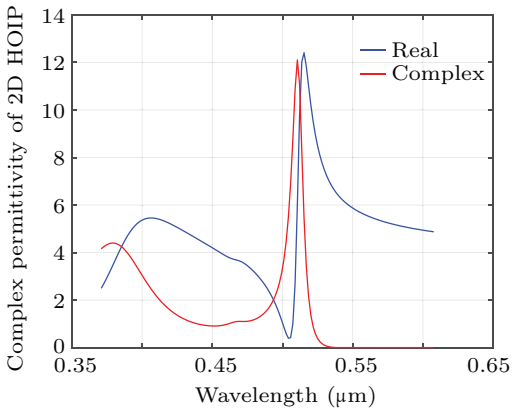


Fig. 2. Complex permittivity of 2D HOIP against wavelength. The blue curve represents the real component (permittivity) whereas the orange curve represents the imaginary component (dielectric loss).

Moreover, the 2D HOIP exhibits a favorable characteristic of relatively lower dielectric loss, signifying minimal energy dissipation during electromagnetic wave absorption. The focus will be at the wavelength close to where the first excitonic peak occurs.

3. Results and analysis

In the proposed setup, exciton–polaritons are introduced into the microcavity using a quasi-resonant continuous-wave (CW) laser. Once the injecting laser's parameters, i.e., angle of incidence, frequency, and intensity, have been properly set, the injected photons and the excitons in the active layer can couple strongly, forming Rabi splitting and two dips in the reflection spectrum. The reflectivity of the proposed setup against wavelength is plotted for different values of the incident angle θ_i (i.e., 0°, 10°, 20°, and 30° respectively) as shown in Fig. 3(a). The presence of the 2D HOIP yields two dips that correspond to the phenomenon of Rabi splitting, indicating strong coupling between the confined cavity photons and the excitons in the 2D HOIP. The leftmost dips represent the branch of upper polaritons (UP), while the rightmost dips represent the branch of lower polaritons (LP). From Fig. 3(b), it is realized that the Rabi splitting increases as the incident angle is increased. With an increase in the incident angle, the horizontal-direction momentum of input photons changes, leading to a modified interaction between the excitons and photons in the active layer. This interaction causes a widening of the separation between the branches, thereby increasing the Rabi splitting. In the presence of OSE, the excitonic energy is expressed as $\omega_x = \omega_x^0 + \delta$ where ω_x^0 is the excitonic energy that is free to flow and δ is the OSE-induced energy shift. δ is directly proportional to the intensity of the Stark optical pulse (square of the field, $|E_o|^2$), and inversely proportional to the photon–exciton detuning, Δ. In the presence of the OSE, expanding the expression for the excitonic energy being[23]

$$\omega_x = \omega_x^0 + \frac{M_{dm} \times |E_o|^2}{2\Delta},$$

where M_{dm} is the dipole moment matrix. The extended Gross–Pitaevskii equation[24] in Eq. (1) is used to model the system's

dynamics and characterize the system's interactions.

$$\mathrm{i}\hbar\partial_t \begin{pmatrix} \psi_\mathrm{x} \\ \psi_\mathrm{c} \end{pmatrix} = \begin{pmatrix} 0 \\ E \end{pmatrix} + \left[\hat{H}_\mathrm{o} + \begin{pmatrix} g_\mathrm{x}|\psi_\mathrm{x}|^2 & 0 \\ 0 & 0 \end{pmatrix}\right] \begin{pmatrix} \psi_\mathrm{x} \\ \psi_\mathrm{c} \end{pmatrix},$$
$$\hat{H}_\mathrm{o} = \hbar \begin{pmatrix} \omega_\mathrm{x}^0 - \mathrm{i}\gamma_\mathrm{x} & \Omega_\mathrm{R}/2 \\ \Omega_\mathrm{R}/2 & \omega_\mathrm{c} - \mathrm{i}\gamma_\mathrm{c} \end{pmatrix}, \quad (1)$$

where γ_x is the excitonic decay rate, and γ_c is the photonic decay rate. ψ_x is the excitonic field, ψ_c is the photonic field, g_x is the exciton–exciton interaction strength, Ω_R is the Rabi frequency, ω_c is the photonic energy, and $\hat{H}_\mathrm{o}$ denotes the Hamiltonian matrix. For brevity, the decay rates and the nonlinear terms have been excluded from the simulation. As a result of the Rabi frequency Ω_R , the LP and UP branches become the two main eigenmodes of $\hat{H}_\mathrm{o}$ as shown below:

$$E_\mathrm{UP,LP}(k) = \frac{\hbar}{2}\left[\omega_\mathrm{c}(k) + \left(\omega_\mathrm{x}^0 + \delta\right) \pm \sqrt{\Omega_\mathrm{R}^2 + \left(\omega_\mathrm{c}(k) - \left(\omega_\mathrm{x}^0 + \delta\right)\right)^2}\right], \quad (2)$$

δ is expressed as $\frac{M_\mathrm{dm}\times|E_\mathrm{o}|^2}{2\Delta}$. The OSE coupled to the proposed setup can be described by a 4×4 Hamiltonian matrix, $\hat{H}_\mathrm{o}$ belonging to the exciton and photon as shown below:

$$\hat{H}_\mathrm{o} = \begin{pmatrix} \omega_\mathrm{c}^\mathrm{o}(k) & \Omega_\mathrm{R}/2 & 0 & 0 \\ \Omega_\mathrm{R}/2 & \omega_\mathrm{x}^\mathrm{o} + \delta & 0 & 0 \\ 0 & 0 & \omega_\mathrm{c}^\mathrm{o}(k) & \Omega_\mathrm{R}/2 \\ 0 & 0 & \Omega_\mathrm{R}/2 & \omega_\mathrm{x}^\mathrm{o} + \delta \end{pmatrix}. \quad (3)$$

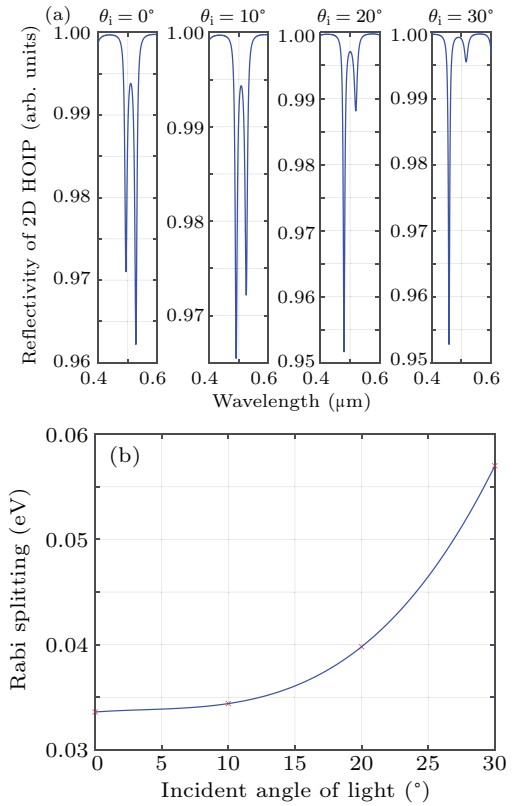


Fig. 3. Reflectivity of the microcavity with 2D HOIP present. (a) Reflectivity against wavelength. (b) Rabi splitting for the different incident angles. The plots represent different incident angles θ_i (i.e., 0°, 10°, 20°, and 30°) from left to right respectively. The left dips represent the UP and the right dips represent the LP.

Alternatively, $M_\mathrm{dm} = \sqrt{(eh/\omega_\mathrm{x}^\mathrm{o})^2 \times E_\mathrm{g}/2m_\mathrm{e}}$,[25] where e is the electron charge, h is the Planck's constant, E_g is the band gap of the quasi-particle, and m_e is the effective electron mass. In this paper, E_g is taken to be 2.3 eV, M_dm is taken to be 1.2×10^{-9} C·m and this gives room for the study of polariton dispersion as the intensity of the optical Stark pulse, $|E_\mathrm{o}|^2$, changes. The curves in Fig. 4 show that the OSE causes a shift in energy levels of the UP and LP branches to a higher level which implies that the dispersion properties of polaritons can be controlled using OSE by varying $|E_\mathrm{o}|^2$. Also, it is observed that $|E_\mathrm{o}|^2$ values in megavolts (MV) are required to shift the energy of the UP and LP branches by milli electronvolts (meV) for a Δ value of 0.2 meV. In the strong coupling region, the Hopfield index of the photons, $C(k)$, and excitons, $X(k)$, satisfy the relationship $|C(k)|^2 + |X(k)|^2 = 1$. In Fig. 5, the excitonic and photonic fractions are plotted for different values of $|E_\mathrm{o}|^2$. It is observed that, as the value of $|E_\mathrm{o}|^2$ increases, the anti-crossing points also increase for a larger value of k, causing a wider separation between the fractions caused by the OSE.

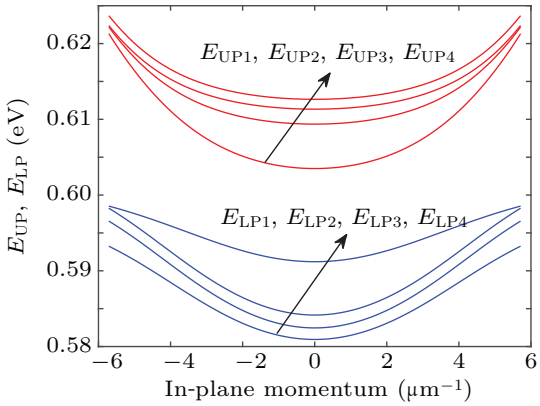


Fig. 4. Dispersion of the UP and LP branches as a function of the in-plane momentum. The Stark-induced energy levels, $E_\mathrm{LP1,UP1}$, $E_\mathrm{LP2,UP2}$, $E_\mathrm{LP3,UP3}$, and $E_\mathrm{LP4,UP4}$ correspond to $|E_\mathrm{o}|^2$ values of 0, 50, 100, and 150 MV respectively.

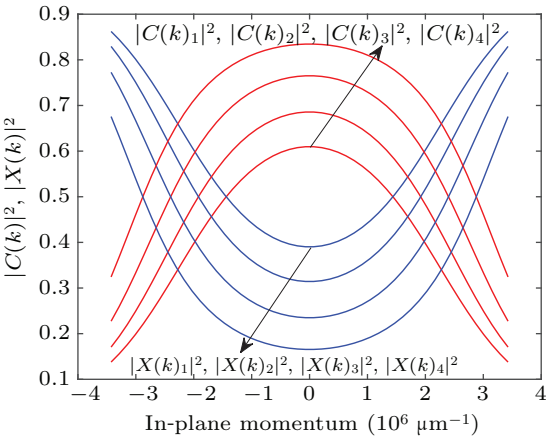


Fig. 5. Changes in photonic and excitonic fractions. $|C(k)_1|^2|X(k)_1|^2$, $|C(k)_2|^2|X(k)_2|^2$, $|C(k)_3|^2|X(k)_3|^2$, and $|C(k)_4|^2|X(k)_4|^2$, correspond to $|E_\mathrm{o}|^2$ values of 0, 50, 100, and 150 MV respectively.

The OSE can happen in a fast transient, paving the way for the dynamic control of the polaritonic field as seen in Fig. 6. In the dynamic analysis, equation (1) is numerically solved using the Runge–Kutta method to the fourth-order.[18] The analysis is done for two cases: when the optical Stark pulse is absent and when the optical Stark pulse is present, considering the excitonic fraction as an example. A transient optical Stark pulse which is of the structure $E = A\exp\left(\left(\frac{t-t_c}{\beta}\right)^2\right)$[19] with a Gaussian shape is applied to the field. A is the amplitude of the pulse, t_c is the center of the pulse (time at which the pulse reaches the maximum value), and β is the pulse width. In the analysis, $A = 3$ V, $t_c = 0.46$ ps, and $\beta = 0.125$ ps. The time domain waveform clearly showing the energy shift in the polaritonic field as a result of the introduction of the optical Stark pulse is seen in Fig. 6(a). The highlighted area shows a peak value at the said transient and this is as a result of the influence of the OSE. The fast Fourier transform (FFT) is then employed to plot the dispersion of the polaritons in the frequency domain of the polaritonic field, shown in Fig. 6(b). The blue curve in Fig. 6(b) represents the case when the OSE is absent. The leftmost peak represents the UP branch whereas the rightmost peak represents the LP branch. In the presence of the OSE (area highlighted with red), an energy shift and numerous frequency points are seen for the polariton branches. Since the optical Stark pulse with Gaussian shape is a superposition of different frequency components, when the pulse interacts with the field, different energy transitions are excited. This excitation leads to the generation of new frequency components. The field's response to the introduction of the Gaussian-shaped optical Stark pulse exhibits resonance with the polariton branches. This resonance results in different frequency components corresponding to the energy differences associated with the polariton branches. These oscillations show different frequencies that correlate to the energy differences. Depending on the amplitude and timing of the pulse, different energy shifts and states can be realized offering opportunities for controlling and manipulating polaritonic properties in a highly tunable manner. For clarity, the values of certain key parameters used in this study have been presented in Table 1.

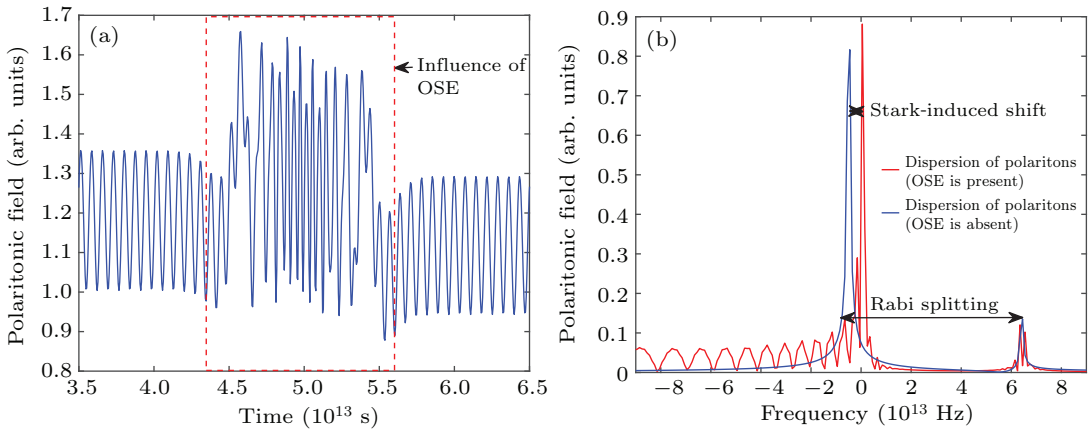


Fig. 6. Dynamic analysis of the OSE on the polaritonic field. (a) Time domain waveform showing the influence of the OSE. (b) Frequency domain showing the dispersion of polaritons and energy shift of the UP (leftmost peaks) and LP (rightmost peaks) branches in the absence and presence of the OSE.

Table 1. Key parameters and their values in the simulation.

Symbol	Parameter	Value
γ_x	excitonic decay	0
γ_c	photonic decay	0
Ω_R	rabi frequency	25 meV
Δ	photon–exciton detuning	0.2 meV
E_g	quasi-particle bandgap	2.3 eV
M_{dm}	dipole moment matrix	1.2×10^{-9} C·m
A	amplitude of the pulse	3 V
t_c	center of the pulse	0.46 ps
β	pulse width	0.125 ps

4. Conclusion

This study has explored the optical properties of 2D HOIP materials and investigated the impact of the OSE on exciton–polaritons within a 2D HOIP active layer. Through steady and dynamic state analyses, the study demonstrated that an external optical Stark pulse effectively modifies various polariton characteristics, including dispersion, excitonic and photonic fractions, and energy levels. The results revealed that the OSE induces energy shifts in excitons proportional to the pulse intensity, leading to significant changes in the polaritonic field. The dynamic state analysis showed a transient fluctuation of the polaritonic field as a result of the influence of the OSE in the time domain and a distinctive energy shift in the Fourier domain. These analyses indicate the nonlinear and complex nature of the field's response to the OSE which is essential for studying the dynamics and behavior of polaritons in optoelectronic devices, microcavities, and other related systems. These findings have significant bearings for the development of optoelectronic devices utilizing 2D HOIP materials. The results provide valuable insights for future research in this rapidly evolving field.

Acknowledgements

The authors would like to express their gratitude to the Key Laboratory of Optical Fiber Sensing and Communication, University of Electronic Science and Technology of China, Ministry of Education of China.

Project supported by the National Natural Science Foundation of China (Grant Nos. 11974071 and 62375040) and the Sichuan Science and Technology Program (Grant Nos. 2022ZYD0108 and 2023JDRC0030).

References

[1] Chen Q Y, Huang Y, Huang P R, Ma T, Cao C and He Y 2016 *Chin. Phys. B* **25** 027104
[2] Jiang M, Deng N, Wang L, Xie H and Qiu Y 2018 *Chin. Phys. B* **27** 067102
[3] Neogi I, Bruno A, Bahulayan D, Goh T W, Ghosh B, Ganguly R, Cortecchia D, Sum T C, Soci C, Mathews N and Mhaisalkar S G 2017 *ChemSusChem* **10** 3765
[4] Yang Y, Lou F and Xiang H 2021 *Nano Lett.* **21** 3170
[5] Wang J, Lu H, Pan X, Xu J, Liu H, Liu X, Khanal D R, Toney M F, Beard M C and Vardeny Z V 2020 *ACS Nano* **15** 588
[6] Kim D, Vasileiadou E S, Spanopoulos I, Kanatzidis M G and Tu Q 2021 *ACS Appl. Mater. Interfaces* **13** 31642
[7] Li W, Wang Z, Deschler F, Gao S, Friend R H and Cheetham A K 2017 *Nat. Rev. Mater.* **2** 16099
[8] Ji L J, Sun S J, Qin Y, Li K and Li W 2019 *Coord. Chem. Rev.* **391** 15
[9] Liu X, Galfsky T, Sun Z, Xia F, Lin E C, Lee Y H, Kéna-Cohen S and Menon V M 2014 *Nat. Photon.* **9** 30
[10] Dufferwiel S, Lyons T P, Solnyshkov D D, Trichet A A, Withers F, Schwarz S, Malpuech G, Smith J M, Novoselov K S, Skolnick M S and Krizhanovskii D N 2017 *Nat. Photon.* **11** 497
[11] Fraser M D 2017 *Semicond. Sci. Technol.* **32** 093003
[12] Sanvitto D and Kéna-Cohen S 2016 *Nat. Mater.* **15** 1061
[13] McGhee K E, Putintsev A, Jayaprakash R, Georgiou K, O'Kane M E, Kilbride R C, Cassella E J, Cavazzini M, Sannikov D A, Lagoudakis P G and Lidzey D G 2021 *Sci. Rep.* **11** 20879
[14] Kaur S, Yao B, Gui Y S and Hu C M 2016 *J. Phys. D: Appl. Phys.* **49** 475103
[15] Zhang W L, Li X J, Wang S S, Zheng C Y, Li X F and Rao Y J 2019 *Nanoscale* **11** 4571
[16] Thao D N, Phuoc D D and Quang N H 2017 *Semicond. Sci. Technol.* **32** 025014
[17] Panna D, Landau N, Gantz L, Rybak L, Tsesses S, Adler G, Brodbeck S, Schneider C, Höfling S and Hayat A 2019 *ACS Photon.* **6** 3076
[18] Shahzadi M, Zhang W L and Khan M T 2019 *Chin. Opt. Lett.* **17** 020014
[19] Zheng C, Zhang Y and Zhang W L 2023 *ACS Appl. Mater. Interfaces* **15** 4764
[20] Tremblay M H, Bacsa J, Zhao B, Pulvirenti F, Barlow S and Marder S R 2019 *Chem. Mater.* **31** 6145
[21] Song B, Hou J, Wang H, Sidhik S, Miao J, Gu H, Zhang H, Liu S, Fakhraai Z, Even J and Blancon J C 2021 *ACS Mater. Lett.* **3** 148
[22] DeCrescent R A, Venkatesan N R, Dahlman C J, Kennard R M, Chabinyc M L and Schuller J A 2019 *ACS Nano* **13** 10745
[23] Dhanabalan S C, Ponraj J S, Zhang H and Bao Q 2016 *Nanoscale* **8** 6410
[24] Hu H and Liu X J 2020 *Phys. Rev. A* **102** 043302
[25] Sie E J, Mclver J W, Lee Y H, Fu L, Kong J and Gedik N 2016 *Proceedings in Defense and Security, Ultrafast Bandgap Photonics*, April 17–21, 2016, Baltimore, USA, p. 129